Current and emerging upper respiratory *in vitro* models to determine *in vitro-in vivo* correlation of inhalation products

Realistic and physiologically relevant *in vitro* models of the nose and mouth-throat have the potential to enhance *in vitro-in vivo* correlation (IVIVC) and reduce the time required for inhaled drug product development.

Zara Sheikh, PhD[a,b,e], Hui Xin Ong, PhD[a,b,c], Paul M. Young, PhD[a,b,d] and Daniela Traini, PhD[a,b,c]
[a]Ab-Initio-Pharma
[b]Respiratory Technology, Woolcock Institute of Medical Research
[c]Macquarie Medical School, Macquarie University
[d]Macquarie Business School, Macquarie University
[e]School of Pharmacy, Brac University

Editor's note: This discussion of nose and mouth-throat models is representative but not comprehensive and no preference or endorsement is intended.

Introduction

The upper respiratory tract, comprising the nose and oropharyngeal regions, has gained widespread interest in pharmaceutical science due to its potential as a non-invasive route for drug delivery. This region's rich vascularization facilitates efficient drug permeation and rapid absorption, enabling swift onset of action. Additionally, it bypasses hepatic first-pass metabolism, reducing systemic side effects and enhancing patient compliance [1]. The nasal cavity has a complex structure corresponding to approximately a surface area of 160 cm^2 and a volume of 15 mL, with specific anatomical regions that should be targeted for certain groups of drugs (Figure 1). The nasal cavity is divided into two fossae by the nasal septum and each fossa extends from the vestibule of the nose and the nasopharynx [2-4]. There are three turbinates (superior, middle and inferior) behind the vestibule and along each outer wall, which act as anatomical targets for locally-acting corticosteroids and antibiotics [2] and therapeutics intended for systemic action [3]. The olfactory region of the nasal cavity situated beside and above the superior turbinate is connected to the brain via the olfactory axonal projections, creating a significant pathway for targeted drug delivery directly from the nose to the brain [5]. The frontal, maxillary and anterior ethmoidal sinuses represent the therapeutic regions of interest for sinus targeting [2]. The upper portion of the rhino pharynx is the primary lymphatic drainage part of the nose, rendering it an attractive target for vaccine delivery [4]. Therefore, in addition to targeting the nose, nasal drug delivery could be used for targeting the brain and the immune system (via vaccines) and for other systemic effects.

Numerous *in vitro* cellular models, excised animal/human nasal mucosa and *in vivo* animal models have been used to study nasal drug deposition. However, there are many disadvantages associated with the use of such *in vivo* animal models and excised nasal mucosa. These include ethical considerations and interspecies variability due to

Figure 1

Schematic representation of nasal cavities showing therapeutic target regions.

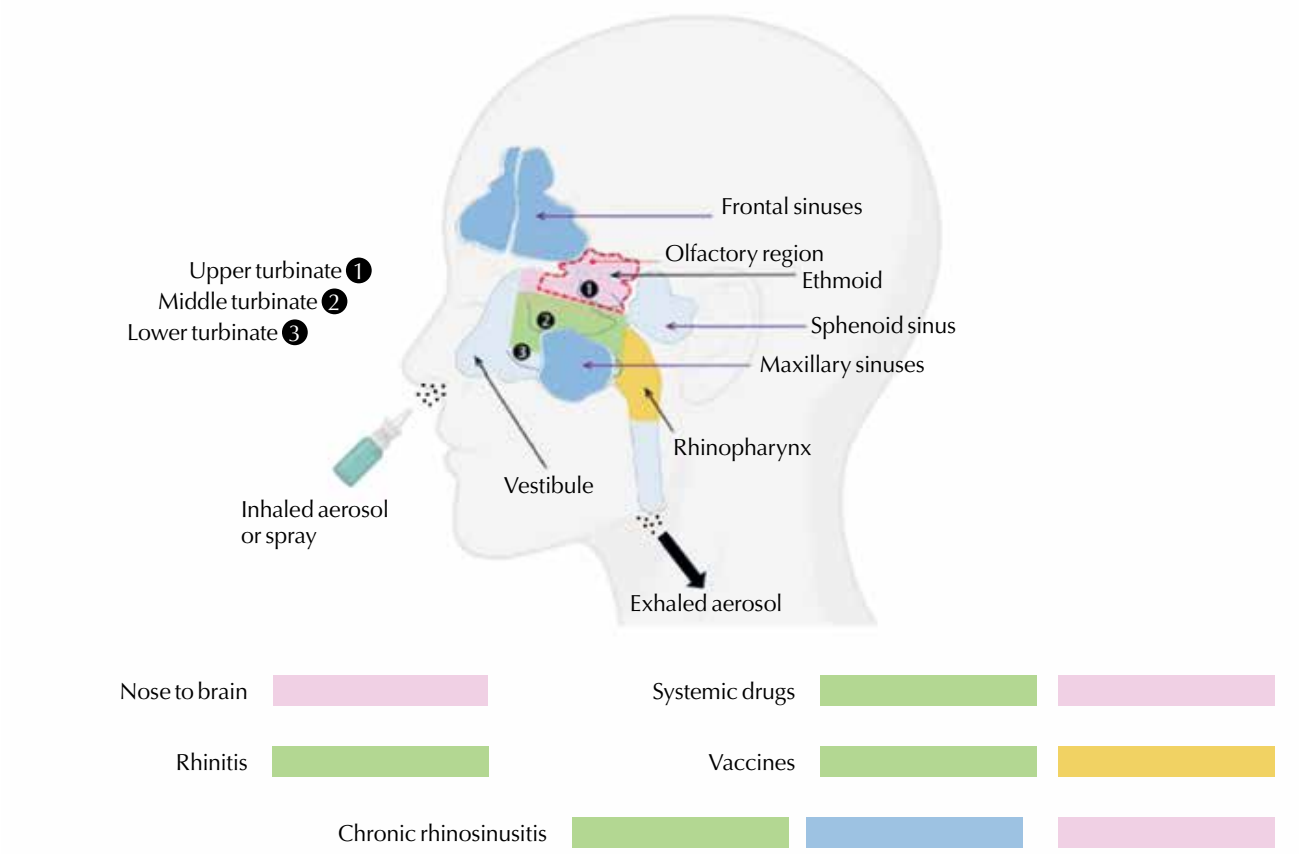

anatomical and physiological differences between animals and humans, which may lead to inaccurate result interpretation and comparison [6]. In this context, *in vitro* nasal anatomical models that are more physiologically representative of the nasal cavity can be of fundamental importance to study nasal drug deposition and predict *in vitro-in vivo* correlation (IVIVC), a regulatory requirement for the development of inhalation products [7].

In vitro assessment of nasal drug delivery

The *in vitro* assessment of nasal drug products is centered around measurements of particle size distribution and delivered dose. The performance of nasal sprays is assessed in accordance with the regulatory requirements of the European Medicines Agency (EMA), the United States Food and Drug Administration (US FDA) or recommendations of the pharmacopeias [8]. Shot weight measurements of nasal solutions, by weighing single actuations, provide an estimate about the consistency of the dose delivered but do not reflect the delivered dose. Therefore, the delivered dose is measured by spray actuation in a suitable container, then the content is assayed to determine the mass of active compound delivered per dose [8]. Droplet size distribution (DSD) is evaluated at two distances from the actuator orifice using laser diffraction and results are interpreted as D10, D50 and D90 corresponding to the 10th, 50th and 90th percentile of particles in the respective formulations. Particle size distribution is found to be similar in terms of volume and drug mass for a liquid solution, however, it could be different for a liquid suspension or powder. Therefore, new tools such as Morphologically-Directed Raman Spectroscopy (MDRS) can be employed to characterize particle size and shape for nasal suspensions and some powders [9].

Cascade impactors are used for drug quantification and for measuring the aerodynamic diameter of the aerosol collected on a set of impaction plates arranged in series [10]. For nasal drug delivery, drug quantification and particle size are measured using a cascade impactor attached to a glass expansion chamber and a pre-separator; however, the relevance of this set-up may be questionable in terms of its volume and geometry in comparison to nasal cavities, as the glass expansion chamber has an approximate volume greater than 2 L [11, 12]. To assess spray pattern and plume geometry, imaging methods are used as per regulatory guidelines. Alternative methods include the use of a USP induction port for drug collection, modified along the segmented induction port. This reflects the distribution of the angle of the droplets emitted

Table 1

Nasal anatomical models used for *in vitro* deposition studies

Model Type	Model Name	Modeling process /Material	Specifications	Reference
Human geometry	Head cadaver	Cadaver specimens with no specific preparation	• One part • Complete anatomical structures • Models with surgery available • Poor preservation	[30, 31]
	Plastinated head model	Plastination of head cadaver/Polymers	• One part • Complete anatomical structures • Exterior access to maxillary sinuses (MS) • Reusable/washable • 6 months to obtain specimen • Validated for nasal resistance and geometry (CT scan)	[32, 33]
Simplified geometry	Glass sinus	Conventional manufacture/Glass	• One part (tube with one simulated sinus) • Transparent and reusable	[34]
	Sinus/Nasal model	Conventional manufacture/Plastic	• Two parts (tube and syringe sinus) with variable geometry • Detachable model • Transparent and reusable	[18]
	ENT anatomical model	Conventional manufacture/Plastic	• Two parts (one square fossae and one simulated MS) • Transparent and reusable	[35]
	PARI nasal cast	Polyoxyethylene	• Eight parts (two plastic fossae with simulated turbinates and glass vials for paranasal sinuses) • Detachable model • Transparent and reusable • Variable geometry	[36, 37]
Advanced with incomplete geometry	3D Systems Viper® SLA printer	Stereolithography (resin)	• One part (no paranasal sinuses) • Transparent and reusable	[38]
	Koken model (Koken Co. Ltd.)	Method not described (silicone resin)	• Two parts (geometry containing turbinates and olfactory region/detachable) • Transparent and reusable • Can be used with medical lubricants Reckitt Benckiser KY®, Arkema Sar-Gel®, KolorCut	[39-41]
	Idealized nasal geometry	Stereolithography (plastic)	• One part (MS excluded, reduced ethmoid) • Transparent and reusable	[42]
	Nasal replica cast (derived from VIPER)	Stereolithography (resin polymerization)	• Six parts (regional section, like Viper model) • Detachable and reusable	[43]
	Human nasal replica cast	Stereolithography (material not mentioned)	• Two parts (sections designed for olfactory depositions) • Detachable and opaque model • Can be coated with layer of 2% w/v mucin solution	[44]
	Nose sinus cast	Stereolithography (polypropylene Stratasys® VeroClear®)	• Five regional sections (three MS) • No frontal and sphenoid sinuses • Detachable and reusable	[45]
	VCU nasal model		• Two parts • Transparent, detachable	[46]
	Nasal cast (Boehringer Ingelheim)	Stereolithography (material not described)	• Five parts (regional section) • Opaque, detachable	[47]
	Realistic nose-throat (RDD model)	Provided in Dassault Systemems SolidWorks® (EASM or EPRT) file formats for free downloading	• One part (incomplete geometry) • Transparent, detachable • 5 years' geometry including nasal cavity, pharynx and larynx, ~22.3 cm3	[48]

(continued)

Table 1 continued

Nasal anatomical models used for *in vitro* deposition studies

Model Type	Model Name	Modeling process /Material	Specifications	Reference
Advanced with complete geometry	Nasosinus model	With the assistance of Koken Co. Ltd. (silicone resin)	• Built from nasal cavity of a cadaver—MS and ethmoid casts (built from adult male CT scan)	[37]
	Saint model (Sophia anatomical infant nose-throat)	Stereolithography (liquid monomer resin, Stereocol)	• One-part • Opaque, reusable • Built from 3D scan of 9-month-old caucasian female patient	[26, 27]
	Models of infant nasal geometry	Stereolithography (acrylic plastic)	• One-part, opaque model • Built from 3D scan of infants (9 geometries, age 3-18 years) -including larynx and MS if present	[28]
	PrINT model (Premature infant nose throat-model)	Stereolithography (photopolymer termed Stratasys® FullCure® 720)	• One-part • Built from MRI scan of a preterm infant (32 weeks) • Transparent and stiff • Validated by CT scan for its geometry	[49]
	Nasal replica (from plastinated head model)	Stereolithography (non-porous resin)	• One part (closed model) • Built from 3D scan of plastinated head model • Exterior access to MS	[25]
	APTAR/UoT/ DTF model	Stereolithography (epoxy plastic and silicone)	• Four parts (axial sections) • Based on CT scan of plastinated head model	[29]
	Nasal airway models	Stereolithography (3D Systems Accura® ClearVue®, plastic meeting USP ClassVI (medical grade)	• Five parts (regional sections) • Geometry including throat and oral cavity • Built from CT scan of toddler (2-year-old), child (5-year-old) and adult (50-year-old). Printed with high resolution for turbinate and olfactory regions, standard resolution for all others. • Transparent and stiff • Detachable and no deformity	[50]
Current standard *in vitro* model	Alberta Idealised Nasal Inlet (AINI)	Manufactured from aluminum	• Four parts (vestibule, turbinates, olfactory region, nasopharynx) • Built from CT and MRI scans of wide range of patient population • Smooth, uniform internal geometry • Easily detachable	[51]

from the nozzle to determine mass median plume angle, which corresponds to the angle where 50% of the drug is deposited [13]. Particle velocity is also an important characteristic for nasal sprays. For instance, Phase-Doppler anemometry has been used for simultaneous measurement of droplet size and velocity as well as particle image velocimetry and particle/droplet image analysis [14]. Even though these *in vitro* methods are available, no single method comprehensively characterizes a nasal spray and reflects the multifactorial complexity of nasal drug administration linked to the physiology of nasal airways to predict intranasal drug deposition, warranting the need for nasal anatomical models as a preclinical tool to determine specific regional nasal deposition [8].

Emergence of various in vitro nasal anatomical models and current models

The modeling of nasal cavities has been extensively used as an *in vitro* tool that closely mimics the upper airway geometry of the human anatomy to study the deposition of nasally inhaled drugs [8]. Initially, nasal airway models were made from human cadaver specimens by using preservation methods (Table 1). However, these cadaver-based casts or digitized copies of the casts showed inaccurate geometries such as expansion in airway passage volume due to post-mortem changes [15]; furthermore, preservation issues and tissue retractions limit the use of such models [16]. The first nasal anatomical model was developed using glass, consisting of a simple tube with two openings (representing the nasal fossae), communicating with a sinus model [17]. A number of similar models have been developed recently with simplified geometry by modeling the nasal fossae with plastic tubes [18, 19] or bottles [20] or by using a plastic cavity with simulated turbinates. Narrow openings and parallel cavities could also be used in these models, using glass vials or syringes to simulate paranasal sinuses [21]. However, these models reflect the basic anatomical structures and do not give an accurate representation of internal nasal structures in detail.

Three-dimensional (3D) printing technology has proved to be a more suitable method for replicating nasal cavity structures to develop nasal anatomical models with higher precision [22]. Advanced models are prepared from 3D human computerized

tomography (CT) scans or magnetic resonance imaging (MRIs) using a 3D-printing method simulating the lines and volumes of the human nasal cavities, closely resembling human geometry and accounting for greater *in vivo* representation (Table 1). 3D printing can offer a faster, simpler and more cost-effective approach that can be automated. Printing time can be optimized by adjusting the scale of the prints, the printer nozzle size and the layer thickness. [23]. These 3D-printed nasal models are usually constructed by stereolithography using fused plastic deposition [24] or resin polymerization [25]. 3D printing is particularly valuable for pediatric upper airway studies, as it provides an ethical alternative to *in vivo* research in children that necessitates stringent ethical considerations and protocols [26-29].

Importantly, the Alberta Idealised Nasal Inlet (AINI), which is an aluminum commercial version of an idealized geometry nasal airway geometry (Copley Scientific, Nottingham, UK) built from CT and MRI scans of a diverse range of patient groups, is currently used as the standard *in vitro* nasal model for representative testing of nasal deposition [52]. It is composed of four separate parts—vestibule (nostrils), turbinates, olfactory region and nasopharynx—that accurately mimic deposition behavior in each region. The AINI is chemically compatible with a range of solvents, allowing simple and quick drug recovery for assay [53]. It has been found that the AINI is more reflective of physiological behavior when its smooth internal surfaces are coated with a surfactant to mimic the presence of mucus within the nasal cavities [54]. Recent studies have shown that the AINI serves as an effective surrogate for regional deposition *in vivo*, demonstrating strong agreement with previous *in vivo* data and thereby enhancing IVIVC. [55].

In vivo methods for assessment of nasal drug deposition

Due to the complexity of the nasal anatomy and the diversity of drug targets, surrogate markers of biological efficacy can be used as *in vivo* methods to assess nasal drug deposition, helping to bridge the gap between *in vitro* assessments and clinical efficacy. Techniques such as radiolabeling external anatomical landmarks and estimating nasal cavity size through acoustic rhinometry could be used to quantify regional nasal deposition more precisely [56]. A combination of two-dimensional (2D) gamma scintigraphy with anatomic imaging techniques, such as magnetic resonance imaging (MRI) or radioactive gas ventilation scintigraphy [57, 58], can be used to enhance the accuracy of predicting regional drug deposition within the nose. Additionally, 3D methods like single photon emission computed tomography (SPECT/CT) with sprayed tracers and positron emission tomography (PET) are currently employed for precise drug labeling and quantification of nasal deposition [59, 60].

In vitro-in vivo correlation of nasal models

Several *in vitro* studies using different types of nasal anatomical models, as well as *in vivo* studies using radiolabeled aerosol deposition [61] or indirect biological measurements such as nasal resistance [62], have shown strong IVIVC for intranasal drugs [58]. Key determinants of total nasal deposition efficiency include particle characteristics, ventilation and nasal anatomy. According to FDA and EMA guidelines, the particle size for intranasal drugs should be greater than 10 µm (typically in the range of 20-100 µm) to avoid lung deposition [63]. Air flow is a critical factor in IVIVC studies, as it significantly influences nasal deposition. Although past studies have suggested that nasal turbinate deposition efficiency did not change significantly with increase in air flow rates from 0 to 20 to 60 L/min [64], recent studies have reported that adjunct air flow can enhance nasal drug transport by 2-3 cm towards the nasopharynx [65]. At higher flow rates, the reduced influence of gravitational sedimentation and inertia may allow particles to penetrate deeper into the olfactory region [66].

Although there is a no general consensus about a standard air flow rate for nasal delivery, studies have commonly used 15-30 L/min as a representative flow rate, depending on the nasal formulation and device [67, 68]. Nasal anatomy also plays a crucial role in intranasal drug deposition, as demonstrated in both *in vitro* anatomical models and *in vivo* deposition studies [8]. Additionally, patient-specific factors, such as the angle of administration, also affect nasal deposition. For example, an *in vitro* study using 10 realistic nasal models showed increased turbinate deposition of cromolyn sodium (from 11% to 73%) when the administration angle decreased from 75º to 30º. However, deposition in upper nasal regions remained poor, highlighting the variability caused by anatomical differences in age, gender and ethnicity [69]. This variability in nasal deposition has been found to be higher in realistic replicas versus those that are idealized, underscoring the need for further validation of the idealized models [70].

While *in vitro* and *in vivo* methods are available for evaluating nasal drug deposition, there is still an unmet need for robust IVIVC models [8, 71, 72]. The lack of standardized deposition studies evaluating the influence of physical parameters on intranasal deposition limits the assessment of IVIVC. To address this, Stoke's equation, which incorporates DSD, air velocity and nasal airway dimension, can be applied to model particle kinetics and deposition patterns [70]. The regions of therapeutic interest also need to be identified prior to conducting IVIVC studies, as the nasal cavity is a complex structure with different dimensions. Further studies need to be performed to determine whether the precise location of drug deposition influences clinical efficacy, thereby

standardizing target regions of interest within the nasal cavity [73].

IVIVC evaluation must also account for the substantial variability between *in vivo* deposition (~100% variability across anatomical regions) compared to *in vitro* variability (~10% for nasal spray characteristics). Furthermore, *in vitro* methods, such as particle characterization, often fail to capture the extent of differences in patient population that lead to *in vivo* deposition variations. In this context, nasal anatomical cast models have proven to be more reliable in terms of simulating the nasal anatomical features, making these models more suitable tools for IVIVC prediction [73]. Additionally, the total mass of drug particles deposited in the nasal cavities per area can be up to 1,000-fold higher compared to the lung, therefore formulation factors related to large delivered doses and post-deposition changes in drug compounds must also be considered in IVIVC evaluation [8].

In vitro assessment of oropharyngeal deposition

Currently, several targeted therapies, including analgesics (lidocaine), antibiotics and mucolytic agents, are delivered to the oropharyngeal region for therapeutic and prophylactic purposes [74]. Still no standardized *in vitro* model exists, underscoring the need to develop more physiologically representative mouth-throat (MT) models to assess *in vitro* oropharyngeal drug deposition and predict therapeutic efficacy.

Physiologically relevant mouth-throat models

Realistic and physiologically relevant mouth-throat models representing upper airways of the human anatomy offer a more accurate prediction of drug deposition in comparison to a simple right-angled impactor inlet, such as the USP inlet (Figure 2). These MT models have been developed using three principal approaches: 1) geometries derived from cadaver casts reported in published literature; 2) reproduction of airway geometries from CT or MRI data of an individual patient or of a group of patients' airways; and 3) idealized geometries including key airway dimensions [73]. As mentioned previously, cadaveric casts can lead to inaccurate estimation of the airway dimensions, making 3D printing based on CT or MRI scans the preferred method, similar to nasal anatomical models [8].

However, MRI data has shown significant variability in dimensions of the oral cavity, oropharynx and larynx across individuals, which are also affected by the type of inhaler device used. These differences are likely attributed to device-induced air flow resistance and variation in patient effort during inhalation [75].

Three main MT models based on oropharyngeal geometries of healthy human subjects include the Oropharyngeal Consortium Mouth-Throats (OPC-MT), Virginia Commonwealth University Mouth-Throats (VCU-MTs) and the Alberta Idealized Mouth-Throat (AIT) (Figure 2) [76].

- The OPC-MT was developed through a collaboration involving AstraZeneca, GlaxoSmithKline and Sanofi-Aventis to represent a broader range of dimensions of both genders [76], with reported internal volumes of 27.6, 91.7 and 84.4 cm^3 for the small, medium and large OPC-MTs, respectively [77]. The higher volume of the medium OPC-MT compared to the large OPC-MT could be based on relative oropharyngeal filtering rather than relative dimensions and complex internal structure [78]. These OPC-MT models have also shown inter-subject variability in oropharyngeal deposition *in vitro* [51, 79].
- The VCU-MT models were developed by Virginia Commonwealth University (US) using resin or polyurethane with internal volumes of 26.6, 61.6 and 96.1 cm^3 for the small, medium and large

Figure 2

Realistic mouth-throat (MT) models. From left: Oropharyngeal Consortium (OPC) large, medium and small MT models; Virginia Commonwealth University (VCU) large, medium and small MT models; Alberta Idealized (AIT) Mouth-Throat model and United States Pharmacopeia (USP) inlet. (Adapted from Wei [77] and reprinted with kind permission.)

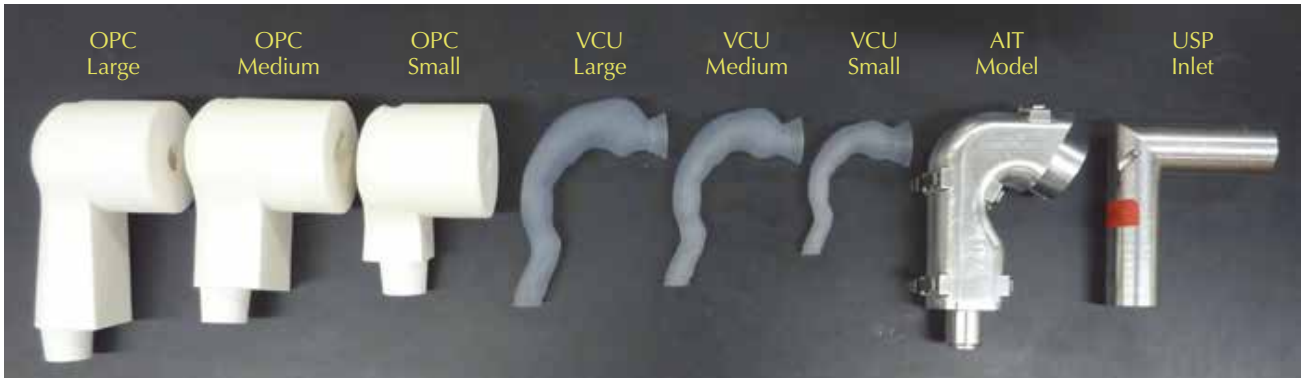

VCU-MT models, respectively, based on CT scans of healthy adults and included anatomical modeling of the trachea to the upper bronchi [80, 81].

- The AIT model, developed by the University of Alberta (Canada) is an idealized geometry based on MRI scans and available published data on airway dimensions [80, 82]. The AIT model is commercially available (Copley Scientific) and is constructed from metal to ensure reproducibility and facilitate drug recovery due to its smooth surface, durability and absence of electrostatic effects. It includes both child and infant models [82]. This model can also be separated into two halves, allowing for a clear distinction between the mouth and pharynx.

The VCU-MT model is more physiologically representative compared to the OPC-MT model, yet it does not include the anatomical features such as the uvula, epiglottis or soft palate. In contrast, the AIT model includes the epiglottis and soft palate but excludes the uvula [83]. Therefore, other non-standardized models including these anatomical features (uvula, epiglottis and soft palate) are currently being investigated to assess the role of these anatomical parts in drug deposition within the MT-region [84]. Additionally, realistic replicas of human airways without the oral cavity and semi-realistic replicas with smooth cylindrical glass walls and bifurcation pieces that include the oral cavity have also been developed. These models highlight the importance of velocity measurements, inspiratory air flow, shape of vocal cords and glottal area in governing the deposition of particles in the oropharyngeal region [85].

In vitro-in vivo correlation of mouth-throat models

To evaluate the performance of the three designs of anatomical MT models, different inhaler devices have been used, including a dry powder inhaler (DPI; Novolizer®, Viatris GmbH & Co. KG, Frankfurt, Germany), an HFA-based pressurized metered dose inhaler (pMDI; Ventolin®, Evohaler®, Glaxo Smith Kline, London, UK) and a soft mist inhaler (SMI; Respimat®, Boehringer Ingelheim, Ingelheim am Rhein, Germany) [78]. Mean drug deposition for the DPI was found to be similar for the VCU-MT, OPC-MT, AIT and USP inlets. However, for the pMDI, greater drug deposition was observed in the VCU-MT and OPC-MT models in comparison to the AIT, which exhibited higher deposition than the USP inlet, although the results were not statistically significant [77]. For the SMI, similar deposition profiles were observed among the VCU-MT, OPC-MT and AIT models, with deposition approximately double that seen with the USP inlet [77, 78].

Recent comparison of *in vitro* results with *in vivo* data (scintigraphy data) showed the significance of inhaler type and inhalation parameters in influencing IVIVC [86, 87]. All MT models (VCU-MT, OPC-MT, AIT) showed good IVIVC for the DPI described above. However, only the VCU-MT and OPC-MT model demonstrated improved IVIVC for the pMDI described above. For the same SMI, all three anatomical MT models showed stronger IVIVC at an inhaled flow rate greater than 100 L/min, which corresponds to the flow rate of an untrained patient. Notably, the OPC-MT was the only MT model to show an improved IVIVC at lower flow rates compared to the USP inlet. Therefore, selecting an anatomical MT model based on the specific drug and inhaler device is essential and conditions must be tested on a product-by-product basis to establish a robust IVIVC [86, 88].

Cell-integrated upper respiratory tract models

Cell-integrated upper respiratory tract models can be pivotal for advancing our understanding of drug delivery and deposition in the nasal cavity and oropharynx. These models can replicate the complex architecture and cellular composition of the upper respiratory tract, enabling a more accurate simulation of physiological conditions compared to traditional *in vitro* systems. By incorporating human respiratory epithelial cells, these models allow for the assessment of drug absorption, metabolism and interaction with the mucosal barrier in a more representative environment. This understanding is potentially important for evaluating the efficacy of intranasal therapies, particularly for conditions such as respiratory infections and neurological diseases. Furthermore, cell-integrated models can be used to investigate specific biological responses to drug formulations, such as inflammation and toxicity, thereby improving their predictive capability for *in vivo* outcomes in terms

Figure 3

3D-printed modified expansion chamber representing the nasal cavity, with an integrated cellular model grown in Snapwells™ (Corning, Inc., Corning, New York, US). (Adapted from Pozzoli, et al. [91] and reprinted with kind permission.)

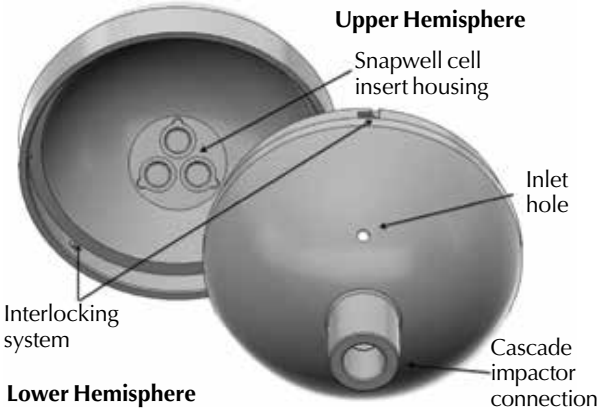

of lower costs and reduced time compared to the use of animal models [89, 90]. Overall, the development of these sophisticated models can enhance the translational potential of research findings and may ultimately lead to more effective and safer therapeutic strategies for patients.

Pozzoli, et al. incorporated an optimized RPMI 2650 nasal cell model into a 3D-printed model of the nose to test deposition and permeation of drugs (Figure 3) [74, 91]. The apparatus, which includes the nasal cell model, was utilized to evaluate a commercial nasal product containing budesonide (Rhinocort®, AstraZeneca, Macquarie Park, NSW, Australia), resulting in high drug deposition, and transport studies were conducted using RPMI 2650 nasal epithelial cells. This novel 3D-printed apparatus, which incorporates cellular components, showed to be a reliable *in vitro* model for testing nasal products under conditions that closely replicate delivery from nasal devices in real-life scenarios.

To mimic the complex anatomy and physiological conditions of the oropharyngeal region, Sheikh, et al. [74] and a research team developed a 3D-printed, *in vitro,* integrated oropharyngeal, air-liquid interface, cellular throat model (Figure 4), incorporating a throat cell line (Detroit 562, ATCC), to study drug transport and absorption in a controlled environment, with the aim of closely simulating *in vivo* conditions. Findings indicated this model can enhance the understanding of drug transport in the oropharynx and may thereby improve the development and optimization of therapeutic formulations targeting this region, offering a tool for preclinical testing and contributing to the design of more effective oropharyngeal therapies.

Figure 4

A. Developed, modified 3D-printed mouth-throat (MT) model with integrated *in vitro* cellular model. B. Lower Snapwell containing cellular model (placed in lower position and shown with black arrow). C. Upper Snapwell with cellular layer (placed in upper position and shown with black arrow). (Adapted from Sheikh, et al. [74] and reprinted with kind permission.)

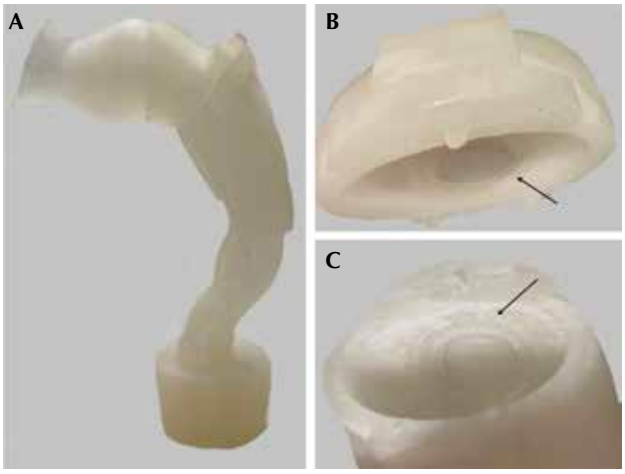

Conclusions

The upper respiratory tract, comprising the nasal cavities and mouth-throat regions, represents a complex and highly variable anatomical structure that poses significant challenges for achieving robust IVIVC. Despite advancements among *in vitro* nasal and mouth-throat models, these systems often fail to fully capture the inherent variability present *in vivo*, such as patient-specific anatomical differences, physiological dynamics and deposition patterns. This limitation is a critical barrier to the accurate prediction of *in vivo* drug deposition and therapeutic outcomes.

Current models range from simplified geometries to advanced 3D-printed constructs that may closely mimic human anatomy based on imaging data. While 3D-printed models represent a significant improvement in physiological relevance and predictive capability, they still lack the ability to replicate dynamic biological processes, such as mucosal clearance, cellular responses and the impact of varied patient physiology. The integration of biomimetic materials and cellular components offers potential for more accurate simulation of drug absorption, metabolism and interaction with respiratory tissues, but these approaches remain under development.

Future research should focus on addressing these limitations by incorporating real-time imaging, dynamic flow conditions and cellular functionality into *in vitro* systems. Standardization of model design and testing protocols will also be essential to improve reproducibility and regulatory acceptance. Ultimately, the development of sophisticated, physiologically representative *in vitro* models could bridge the gap between laboratory research and clinical applications, enhancing the efficiency and efficacy of therapeutic interventions for respiratory diseases.

References

1. Keller, L.A., et al., Intranasal drug delivery: Opportunities and toxicologic challenges during drug development. Drug Deliv Transl Res, 2022. 12(4): p. 735-757.

2. Laube, B.L., Devices for aerosol delivery to treat sinusitis. J Aerosol Med, 2007. 20 Suppl 1: p. S5-17; discussion S17-18.

3. Anaísa Pires, A.F., et al., Intranasal drug delivery: How, why and what for? J. Pharm Sci, 2009. 12(3): 288-311.

4. Gizurarson, S., Anatomical and histological factors affecting intranasal drug and vaccine delivery. Curr Drug Deliv, 2012. 9(6): p. 566-582.

5. Khan, T.T.S., et al., Intranasal delivery of glucagon-like peptide-1 to the brain for obesity treatment:

Opportunities and challenges. Expert Opin Drug Deliv, 2024. 21(7): p. 1081-1101.

6. Haasbroek-Pheiffer, A., et al., *In vitro* and *ex vivo* experimental models for evaluation of intranasal systemic drug delivery as well as direct nose-to-brain drug delivery. Biopharm Drug Dispos, 2023. 44(1): p. 94-112.

7. Réminiac, F., et al., Nasal high flow nebulization in infants and toddlers: An *in vitro* and *in vivo* scintigraphic study. Pediatr Pulmonol, 2017. 52(3): p. 337-344.

8. Le Guellec, S., et al., *In vitro - in vivo* correlation of intranasal drug deposition. Adv Drug Deliv Rev, 2021. 170: p. 340-352.

9. US Food and Drug Administration. Guidance for industry. Bioavailability and bioequivalence studies for nasal aerosols and nasal sprays for local action. 2003.

10. Mitchell J.P., et al., Laser diffractometry as a technique for the rapid assessment of aerosol particle size from inhalers. J Aerosol Med, 2006. 19: p. 409-433.

11. Doub, W.H., et al., Measurement of drug in small particles from aqueous nasal sprays by Andersen Cascade Impactor. Pharm Res, 2012. 29(11): p. 3122-3130.

12. Williams, G., et al. Evaluation of nasal inlet ports having simplified geometry for the pharmacopeial assessment of mass fraction of dose likely to penetrate beyond the nasopharynx: A preliminary investigation. AAPS PharmSciTech, 2018. 19(8): p. 3723-3733.

13. Moraga-Espinoza, D., et al., A modified USP induction port to characterize nasal spray plume geometry and predict turbinate deposition under flow. Int J Pharm, 2018. 548(1): p. 305-313.

14. Liu, X., et al., Assessment of the influence factors on nasal spray droplet velocity using phase-Doppler anemometry (PDA). AAPS PharmSciTech, 2011. 12(1): p. 337-343.

15. Cheng, K-H., et al., *In vivo* measurements of nasal airway dimensions and ultrafine aerosol deposition in the human nasal and oral airways. J Aerosol Sci, 1996. 27(5): p. 785-801.

16. Durand, M., et al., Preliminary study of the deposition of aerosol in the maxillary sinuses using a plastinated model. J Aerosol Med, 2004. 14: p. 83-93.

17. Kim, C.S., et al., Aerosol deposition in the airway with excessive mucus. J Appl Physiol, 1985. 59(6): p. 1766-1772.

18. Maniscalco, M., et al., Assessment of nasal and sinus nitric oxide output using single-breath humming exhalations. Eur Respir J, 2003. 22(2): p. 323-329.

19. Moller, W., et al., Nasal high flow clears anatomical dead space in upper airway models. J Appl Physiol (1985), 2015. 118(12): p. 1525-1532.

20. Xi, J., et al., Understanding the mechanisms underlying pulsating aerosol delivery to the maxillary sinus: *In vitro* tests and computational simulations. Int J Pharm, 2017. 520(1-2): p. 254-266.

21. Thieme, S.F., et al., Ventilation imaging of the paranasal sinuses using xenon-enhanced dynamic single-energy CT and dual-energy CT: A feasibility study in a nasal cast. Eur Radiol, 2012. 22(10): p. 2110-2116.

22. Valtonen, O., et al., Three-dimensional printing of the nasal cavities for clinical experiments. Sci Rep, 2020. 10(1): p. 502.

23. Deruyver, L., et al., The importance of pre-formulation studies and of 3D-printed nasal casts in the success of a pharmaceutical product intended for nose-to-brain delivery. Adv Drug Deliv Rev, 2021. Aug: 175.

24. Le Guellec, S., et al., Validation of anatomical models to study aerosol deposition in human nasal cavities. Pharm Res, 2014. 31(1): p. 228-337.

25. Leclerc, L., et al., Impact of airborne particle size, acoustic airflow and breathing pattern on delivery of nebulized antibiotic into the maxillary sinuses using a realistic human nasal replica. Pharm Res, 2014. 31(9): p. 2335-2343.

26. Janssens, H.M., et al., The Sophia anatomical infant nose-throat (Saint) model: A valuable tool to study aerosol deposition in infants. J Aerosol Med, 2001. 14: p. 433-441.

27. Laube, B.L., et al., Deposition of albuterol aerosol generated by pneumatic nebulizer in the Sophia anatomical infant nose-throat (Saint) model. Pharm Res, 2010. 27(8): p. 1722-1729.

28. Storey-Bishoff, J., et al., Deposition of micrometer-sized aerosol particles in infant nasal airway replicas. J Aerosol Sci, 2008. 39(12): p. 1055-1065.

29. Minocchieri S., et al. Development of the premature infant nose throat-model (PrINT-model): An upper airway replica of a premature neonate for the study of aerosol delivery. Pediatr Res, 2008. 64: p. 141-146.

30. Valentine, R., et al., A prospective controlled trial of pulsed nasal nebulizer in maximally dissected cadavers. Am J Rhinol, 2008. 22(4): p. 390-394.

31. Manes, R.P., et al., Prospective evaluation of aerosol delivery by a powered nasal nebulizer in the cadaver model. Int Forum Allergy Rhinol, 2011. 1(5): p. 366-371.

32. Durand, M., et al., Impact of acoustic airflow nebulization on intrasinus drug deposition of a human plastinated nasal cast: New insights into the mechanisms involved. Int J Pharm, 2011. 421(1): p. 63-71.

33. Leclerc, L., et al., Impact of acoustic airflow on intrasinus drug deposition: New insights into the vibrating mode and the optimal acoustic frequency to enhance the delivery of nebulized antibiotic. Int J Pharm, 2015. 494(1): p. 227-234.

34. Guillerm, R., et al., A new method of aerosol penetration into the sinuses. Presse Med (1893), 1959. 67(27): p. 1097-1098.

35. Durand, M., et al., *In vitro* study of sonic aerosol to maxillary sinuses treatment. Drug Delivery to the Lungs 2016. J Aerosol Med. 19(2): p. 221.

36. Möller, W., et al., Ventilation and drug delivery to the paranasal sinuses: Studies in a nasal cast using pulsating airflow. Rhinol, 2008. 46(3): p. 213-220.

37. Saijo, R., et al., Particle deposition of therapeutic aerosols in the nose and paranasal sinuses after transnasal sinus surgery: A cast model study. Am J Rhinol, 2004. 18(1): p. 1-7.

38. Kelly, J.T., et al., Particle deposition in human nasal airway replicas manufactured by different methods. Part I: Inertial regime particles. Aerosol Sci Technol, 2004. 38(11): p. 1063-1071.

39. Kundoor, V., et al. Assessment of nasal spray deposition pattern in a silicone human nose model using a color-based method. Pharm Res, 2010. 27(1): p. 30-36.

40. Guo, Y., et al., The effect of formulation variables and breathing patterns on the site of nasal deposition in an anatomically correct model. Pharm Res, 2005. 22(11): p. 1871-1878.

41. Nižić, L., et al., Innovative sprayable *in situ* gelling fluticasone suspension: Development and optimization of nasal deposition. Int J Pharm, 2019. 563: p. 445-456.

42. Kiaee, M., et al., An idealized geometry that mimics average nasal spray deposition in adults: A computational study. Comput Biol Med, 2019. 107: p. 206-217.

43. Schroeter, J.D., et al., Experimental measurements and computational predictions of regional particle deposition in a sectional nasal model. J Aerosol Med Pulm Drug Deliv, 2015. 28(1): p. 20-29.

44. Yarragudi, S.B., et al., Formulation of olfactory-targeted microparticles with tamarind seed polysaccharide to improve nose-to-brain transport of drugs. Carbohydr Polym, 2017. 163: p. 216-226.

45. Xi, J., et al., Nasal and olfactory deposition with normal and bidirectional intranasal delivery techniques: *In vitro* tests and numerical simulations. J Aerosol Med Pulm Drug Deliv, 2017. 30(2): p. 118-131.

46. Azimi, M., et al. Evaluating simulated patient use in realistic nasal airway models for the *in vitro* characterization of nasal spray products. Inhalation, 2018. 12(1): p. 9-15.

47. Wingrove, J., et al., Characterisation of nasal devices for delivery of insulin to the brain and evaluation in humans using functional magnetic resonance imaging. J Control Release, 2019. 302: p. 140-147.

48. Respiratory Drug Delivery Online. Realistic mouth throat models in three sizes. https://www.rddonline.com/rdd/rdd.php?sid=105.

49. Minocchieri, S., et al., Development of the premature infant nose throat-model (PrINT-model): An upper airway replica of a premature neonate for the study of aerosol delivery. Pediatr Res, 2008. 64(2): p. 141-146.

50. Hosseini, S., et al., *In vitro* measurement of regional nasal drug delivery with Flonase,® Flonase® Sensimist,™ and MAD Nasal™ in anatomically correct nasal airway replicas of pediatric and adult human subjects. J Aerosol Med Pulm Drug Deliv, 2019. 32(6): p. 374-385.

51. Chen, J., et al., Characterizing regional drug delivery within the nasal airways. Expert Opin Drug Deliv, 2024. 21(4): p. 537-551.

52. Chen, J.Z., et al., *In vitro* assessment of an idealized nose for nasal spray testing: Comparison with regional deposition in realistic nasal replicas. Int J Pharm, 2020. 582: p. 119341.

53. Copley Scientific, Realistic throat and nasal cast models. https://www.copleyscientific.com/inhaler-testing/realistic-throat-and-nasal-models/alberta-idealised-nasal-inlet-aini/.

54. Murphy B, et al., Intranasal powder administration of a spray dried tuberculosis vaccine candidate characterized using the Alberta Idealized Nasal Inlet. Respiratory Drug Delivery 2022. 2022. p. 441-446.

55. Chen, J.Z., et al., *In vitro* regional deposition of nasal sprays in an idealized nasal inlet: Comparison with *in vivo* gamma scintigraphy. Pharm Res, 2022. 39(11): p. 3021-3028.

56. Emanuel, I.A., et al., Nasal deposition of ciclesonide nasal aerosol and mometasone aqueous nasal spray in allergic rhinitis patients. Am J Rhinol Allergy, 2014. 28(2): p. 117-121.

57. Möller, W., et al. Topical drug delivery in chronic rhinosinusitis patients before and after sinus surgery using pulsating aerosols. PloS One, 2013. 8, e74991.

58. Vecellio, L., et al., Deposition of aerosols delivered by nasal route with jet and mesh nebulizers. Int J Pharm, 2011. 407(1-2): p. 87-94.

59. Leclerc, L., et al., Assessing sinus aerosol deposition: Benefits of SPECT-CT imaging. Int J Pharm, 2014. 462(1-2): p. 135-141.

60. Corcoran, T.E., Imaging in Aerosol Medicine. Respir Care, 2015. 60(6): p. 850-855; discussion 855-857.

61. Djupesland, P.G. et al., Nasal deposition and clearance in man: Comparison of a bidirectional powder

device and a traditional liquid spray pump. J Aerosol Med Pulm Drug Deliv, 2012. 25(5): p. 280-289.

62. Goh, L.C., et al., Lidocaine/phenylephrine nasal spray versus nebulization prior to nasoendoscopy: A randomized controlled trial. Otolaryngol Head Neck Surg, 2018. 159(4): p. 783-788.

63. Rygg, A., et al., Absorption and clearance of pharmaceutical aerosols in the human nose: Effects of nasal spray suspension particle size and properties. Pharm Res, 2016. 33(4): p. 909-921.

64. Foo, M.Y., et al., The influence of spray properties on intranasal deposition. J Aerosol Med, 2007. 20(4): p. 495-508.

65. Sosnowski, T.R., et al., Impact of physicochemical properties of nasal spray products on drug deposition and transport in the pediatric nasal cavity model. Int J Pharm, 2020. 574: p. 118911.

66. Williams, G., et al., *In vitro* anatomical models for nasal drug delivery. Pharmaceutics, 2022. 14(7): p. 1353.

67. Henriques, P., et al., Amorphous nasal powder advanced performance: *In vitro/ex vivo* studies and correlation with *in vivo* pharmacokinetics. J Pharm Investig, 2023. 53(5): p. 723-742.

68. Gomes Dos Reis, L., et al., Advances in the use of cell penetrating peptides for respiratory drug delivery. Expert Opin Drug Deliv, 2020. 17(5): p. 647-664.

69. Warnken, Z.N., et al., Formulation and device design to increase nose to brain drug delivery. J Drug Deliv Sci Technol, 2016. 35: p. 213-222.

70. Cheng, Y.S., Aerosol deposition in the extrathoracic region. Aerosol Sci Technol, 2003. 37(8): p. 659-671.

71. Newman, S.P., et al., Drug delivery to the nasal cavity: *In vitro* and *in vivo* assessment. Crit Rev Ther Drug Carrier Syst, 2004. 21(1): p. 21-66.

72. Newman, S.P., et al., *In vitro-in vivo* correlations (IVIVCs) of deposition for drugs given by oral inhalation. Adv Drug Deliv Rev, 2020. 167: p. 135-147.

73. Usmani, O.S., et al., Regional lung deposition and bronchodilator response as a function of beta2-agonist particle size. Am J Respir Crit Care Med, 2005. 172(12): p. 1497-1504.

74. Sheikh, Z., et al., The development of a 3D-printed *in vitro* integrated oro-pharyngeal air-liquid interface cellular throat model for drug transport. Drug Deliv Transl Res, 2023. 13(5): p. 1405-1419.

75. Ehtezazi, T., et al., Suitability of the upper airway models obtained from MRI studies in simulating drug lung deposition from inhalers. Pharm Res, 2005. 22(1): p. 166-170.

76. Burnell, P.K.P., et al., Studies of the human oropharyngeal airspaces using magnetic resonance imaging iv—The oropharyngeal retention effect for four inhalation delivery systems. J Aerosol Med, 2007. 20(3): p. 269-281.

77. Wei, X., Development of clinically relevant *in vitro* performance tests for powder inhalers. Virginia Commonwealth University, 2015.

78. Finlay, W., et al. Choosing 3-D mouth-throat dimensions: A rational merging of medical imaging and aerodynamics. Respiratory Drug Delivery 2010.

79. Heenan, A.F., et al., An investigation of the relationship between the flow field and regional deposition in realistic extra-thoracic airways. J Aerosol Sci, 2004. 35(8): p. 1013-1023.

80. Stapleton, K.W., et al., On the suitability of k–ε turbulence modeling for aerosol deposition in the mouth and throat: A comparison with experiment. J Aerosol Sci, 2000. 31(6): p. 739-749.

81. Delvadia, R.R., et al., *In vitro* tests for aerosol deposition. I: Scaling a physical model of the upper airways to predict drug deposition variation in normal humans. J Aerosol Med Pulm Drug Deliv, 2012. 25(1): p. 32-40.

82. Golshahi, L., et al., Use of airway replicas in lung delivery applications. J Aerosol Med Pulm Drug Deliv, 2022. 35(2): p. 61-72.

83. Mitchell, J., et al., Adapting the abbreviated impactor measurement (AIM) concept to make appropriate inhaler aerosol measurements to compare with clinical data: A scoping study with the "Alberta" Idealized Throat (AIT) inlet. J Aerosol Med Pulm Drug Deliv, 2012. 25(4): p. 188-197.

84. Ma, Z., et al., An experimental study of the effect of individual upper airway anatomical features on the deposition of dry powder inhaler formulations. J Aerosol Sci, 2024. 177: p. 106320.

85. Frantisek Lizal, J.J., et al., Investigation of the airflow inside realistic and semi-realistic replicas of human airways. EPJ Web of Conferences. 2015.

86. Hirst, P.H., et al., *In vivo* lung deposition of hollow porous particles from a pressurized metered dose inhaler. Pharm Res, 2002. 19(3): p. 258-264.

87. Brand, P., et al., Higher lung deposition with Respimat Soft Mist inhaler than HFA-MDI in COPD patients with poor technique. Int J Chron Obstruct Pulmon Dis, 2008. 3(4): p. 763-770.

88. Newman, S.P., et al., Lung deposition of Fenoterol and Flunisolide delivered using a novel device for inhaled medicines: Comparison of Respimat with conventional metered-dose inhalers with and without spacer devices. Chest, 1998. 113(4): p. 957-963.

89. Metz, J.K., et al., *In vitro* tools for orally inhaled drug products—State of the art for their application in pharmaceutical research and industry and regulatory challenges. *In Vitro* Models, 2022. 1(1): p. 29-40.

90. Selo, M.A., et al., *In vitro* and *ex vivo* models in inhalation biopharmaceutical research—Advances,

challenges and future perspectives. Adv Drug Deliv Rev, 2021. 177: p. 113862.

91. Pozzoli, M., et al., Application of RPMI 2650 nasal cell model to a 3D printed apparatus for the testing of drug deposition and permeation of nasal products. Eur J Pharm Biopharm, 2016. 107: p. 223-233.

Zara Sheikh, PhD,[a,b,e] is Assistant Professor, School of Pharmacy, Brac University (corresponding author; zara.sheikh@bracu.ac.bd). Hui Xin Ong, PhD,[a,b,c] is COO, Ab-Initio-Pharma. Paul M. Young, PhD,[a,b,d] is CEO, Ab-Initio-Pharma. Daniela Traini, PhD,[a,b,c] is Professor of Respiratory Science, Macquarie Medical School, Macquarie University. [a]Ab-initio-pharma, Sydney, NSW 2113, Australia. [b]Respiratory Technology, Woolcock Institute of Medical Research, Sydney, NSW 2113, Australia. [c]Macquarie Medical School, Faculty of Medicine, Health and Human Sciences, Macquarie University, Sydney, NSW 2113, Australia. [d]Macquarie Business School, Macquarie University, Sydney, NSW 2113, Australia. [e]School of Pharmacy, Brac University, Dhaka 1212, Bangladesh.